CONFERENCE PRE-PRINT

VALIDATION OF PLASMA-WALL SELF-ORGANIZATION THEORY BY HIGH DENSITY LIMITS ACHIEVED ON EAST

J.X. LIU
International Joint Research Laboratory of Magnetic Confinement Fusion and Plasma Physics, State Key Laboratory of Advanced Electromagnetic Technology, Huazhong University of Science and Technology
Wuhan, China
Email: liu_jiaxing@hust.edu.cn

P. ZHU
International Joint Research Laboratory of Magnetic Confinement Fusion and Plasma Physics, State Key Laboratory of Advanced Electromagnetic Technology, Huazhong University of Science and Technology
Wuhan, China
Engineering Physics, University of Wisconsin-Madison
Madison, USA

D.F. Escande
Aix-Marseille Université
Marseille, France

W.B. Liu, N. Yan, L. Zhang, S.W. Xue, J.P. Qian, R. Ding, R.J. Zhou, X. Lin, L. Wang, and the EAST team
Institute of Plasma Physics, Chinese Academy of Sciences
Hefei, China

Abstract

Achieving high electron density is essential for tokamaks to reach energy breakeven and sustain a burning plasma. However, tokamak operation is often constrained by an upper density limit, beyond which disruptions occur. Understanding and overcoming this density limit remains a key challenge. Here, we present experimental results from the EAST tokamak, achieving a line-averaged electron density in the range (1.3-1.65) Greenwald density limit n_G, while the usual range in EAST is (0.8-1.2) n_G. This was achieved through ECRH-assisted Ohmic start-up combined with a sufficiently high initial neutral density. This technique is motivated by and consistent with predictions of a recent plasma-wall self-organization (PWSO) theory, that increasing ECRH power or pre-filled gas pressure leads to lower plasma temperatures around divertor target and higher density limits by mimicking a stellarator start-up. Furthermore, the experiments are confirmed operating within the density-free regime predicted by the PWSO model. These results suggest a promising scheme for substantially increasing the density limit in tokamaks, a critical advancement toward achieving the burning plasma.

1. INTRODUCTION

Achieving high plasma density is essential for satisfying the Lawson criterion in magnetic confinement fusion, yet density limits often constrain tokamak performance, potentially leading to disruptive terminations [1]. Over decades, understanding and predicting these limits remaines a focal point of fusion research. For the past decades, the Greenwald density limit $n_G(\mathrm{m}^{-3}) = I_p(\mathrm{MA}) \times 10^{20}/(\pi a(\mathrm{m})^2)$ has been widely used as an empirical scaling law for tokamak density limit [1]. However, this scaling law does not account for the heating power dependence of the density limit that has been observed in many experiments [2, 3] and confirmed by many theoretical models [4, 5]. Besides, many experiments have exceeded this density limit, such as those on FTU [6], and DIII-D [7].

A recent plasma-wall self-organization (PWSO) theory was built under the assumption that the primary factors influencing the power balance limits stem from impurity radiation, which is largely controlled by plasma-wall interactions [8]. It shows that there are two attraction basins for the density: the density-limit basin corresponding

to a higher target-region plasma temperature, and the density-free basin corresponding to a lower target-region plasma temperature, where the density limit moves up to an extremely high value as the target temperature decreases. Besides, a relatively higher density limit is reached in stellarator when the start-up is performed by using higher ECRH power [9]. This higher density limit might be due to their mode of breakdown at start-up phase: the massive use of ECRH power with high neutral density producing less impurities [8, 10]. Both PWSO theory and stellarator results were an incentive to perform experiments in J-TEXT, which directly validated key aspects of PWSO theory in electron cyclotron resonance heating (ECRH)-assisted Ohmic start-up discharges [11, 12]. Building on the success of these experiments, the EAST tokamak provides a unique platform to extend the validation of the PWSO model. With the tungsten plasma-facing components, the EAST tokamak allows the exploration of PWSO induced density limits under conditions distinct from those of J-TEXT. Indeed, whereas with carbon walls the chemical sputtering is important, for tungsten walls the physical sputtering dominates, which might enable reaching the density-free basin predicted by the PWSO theory.

In this study, we present the EAST experimental results [13], with a detailed analysis on the role of ECRH power and pre-filled gas pressure in achieving high-density regimes. The EAST experimental results show that increasing the pre-filled neutral gas pressure and/or the ECRH power can increase the density limit up to $1.3n_G$ to $1.65n_G$, while the usual range in EAST is (0.8-1.2) n_G [14]. The experimental data for density limit n_c and plasma temperature around divertor T_t are consistent quantitatively with the prediction of PWSO theory. Moreover, as expected, these discharges are found to operate in the density-free regime of PWSO theory, which implies that a substantial enhancement in the density limit of tokamaks may be attainable through achieving detachment without actively introducing impurities.

2. EXPERIMENTAL RESULTS

There are two main series of discharges in our experiments (Table 1), the one with varied pre-filled neutral gas pressure at a fixed ECRH power and the other with varied ECRH heating powers at a fixed pre-filled pressure. We selected a reference discharge #143069 to serve as a point of comparison, which is based on an ECRH-assisted Ohmic start-up scenario similar to those reported in reference [15]. The time history of its key parameters, including total radiation levels, plasma current I_p, ECRH power and line-average electron density n_e, are shown in Fig. 2. This discharge starts at 0.0 s, with a toroidal magnetic field of 2.5 T, a pre-filled gas puffing voltage $V_{\rm gas}$ of about 3 V with the corresponding number of injected deuterium (D_2) of 6.6×10^{19}, an ECRH power of about 600 kW with the pulse width [0.0 s, 4.5 s], and a plasma current of 250 kA. Hydrogen gas is injected as the working gas, and no other kind of gas or impurity is injected throughout the discharge. During the current plateau period, the gas injection continues until the plasma density limit of about 1.5 $n_{\rm G}$ is reached. At this point, the plasma density starts to decrease and then rapidly drops to zero, without any prior manifestation of MHD activities. In the following analysis, the density limit, defined as the maximum density immediately reached prior to the disruption, is taken at the onset of the collapse. The pre-filled gas amount is defined as that of the total injected gas before $t = 0$ s. Other parameters, including the target temperature T_t, effective charge number $Z_{\rm eff}$, and the averaged radiated power, are evaluated as time-averaged values over the interval 5–6 s.

TABLE 1. **Summary of key parameters for the density limit discharges analyzed in this study.** The first column lists the shot numbers. $P_{\rm EC}$ in the second column indicates the applied ECRH power. The third column shows the pre-filled gas amount, which is positively correlated with, and controlled by, the applied pre-fill voltage. The fourth column presents the achieved line-averaged electron density, taken as a measure of the density limit.

shot number (1430xx)	$P_{\rm EC}$ (kW)	Pre-filled gas (D_2) amount (10^{20} molecules)	Density limit (10^{19}m^{-3})
64	0	0.66	4.8
69	600	0.66	5.2
73	600	1.0	5.3
74	600	1.37	5.4
75	600	1.73	5.4
77	0	0.66	5.5
79	600	0.66	5.6
80	600	0.66	5.6

For discharges with varied pre-filled neutral gas and ECRH power of about 600 kW, the experimental results indicate that the density limit increases with the pre-filled gas pressure until saturation (Fig. 3a). This enhancement

of density limit is related to the decrease of total radiation power (Fig. 3b) and the higher plasma cleanliness, as indicated by the effective charge number $Z_{\rm eff}$ (Fig. 3c). The cleanliness of plasma and the enhanced density limit should be mainly influenced by the plasma-wall interaction, which is related to the plasma temperature around the divertor target. This can be inferred from Fig. 3d, which shows the plasma temperature around the low-outer divertor target is lower when the pre-filled gas pressure is higher and the final density limit is higher. For discharges with varied ECRH heating powers and the lowest pre-filled gas pressure of all cases, the experimental results indicate that the density limit weakly increases with the ECRH power. For instance, from shot #143064 to shot #143069, density limit increases from $4.9 \times 10^{19}\mathrm{m}^{-3}$ to $5.2 \times 10^{19}\mathrm{m}^{-3}$ as the ECRH power increases from 0 to 600 kW (Fig. 3). This density limit enhancement is also related to the decrease of total radiation (Fig. 3b), the higher plasma cleanliness (Fig. 3c), and the lower plasma temperature around the low-outer divertor target (Fig. 3d), which can all be attributed to the reduced strength of plasma-wall interaction. The contribution of Ohmic heating can be estimated from the loop voltage measurements shown in Fig. 1. The maximum difference in Ohmic heating power between discharges with and without ECRH is less than 200 kW, which is small compared with the applied ECRH power of 600 kW. Thus the enhanced density limit mainly correlates with the increased ECRH power.

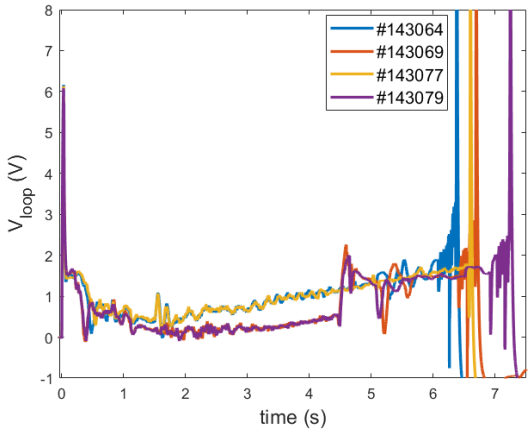

FIG. 1. Loop voltage as functions of time in different discharges.

It is noted that shots #143079 and #143069 have identical input parameters, yet yield different plasma temperature around the divertor target or density limit. A similar observation can be made regarding shots #143064 and #143077. These differences may be due to alterations in wall conditions over time [16], because there are several density limit discharges between shots #143064 and #143079, which can have potential impacts on the wall conditions. The successive effective discharges demonstrate a striking point that the target region plasma temperature T_t and the effective charge number $Z_{\rm eff}$ decreases with discharge number, and the density limit n_e increases with discharge number. This indicates the wall condition is improving with time.

In summary, these experimental results demonstrate that increasing pre-filled gas or/and ECRH power leads to lower plasma temperature around the divertor target and higher density limit well above the Greenwald density limit (Fig. 3d). This enhancement of density limit is related to the improved wall condition. In the following, we will compare the experimental results with the predictions of plasma-wall self-organization theory.

3. COMPARISON WITH PWSO THEORY

PWSO theory describes the plasma-wall interaction through the relationship between sputtered impurities' radiation and heating power [8, 11]. The basic idea of the PWSO theory (section 4.1 of [8]) is that the existence of a time delay in the feedback loop relating impurity radiation and impurity production on divertor/limiter plates yields the following equation in a 0D model

$$R_+ = \alpha(P - R) \tag{1}$$

where P is the total input power to plasma, R the total radiated power, and R_+ the delayed radiation power during the next cycle of the feedback loop. The coefficient α quantifies the radiation power R_+ generated by the impurity produced from the plasma-wall interaction that is proportional to the deposition of the outflow power $(P - R)$

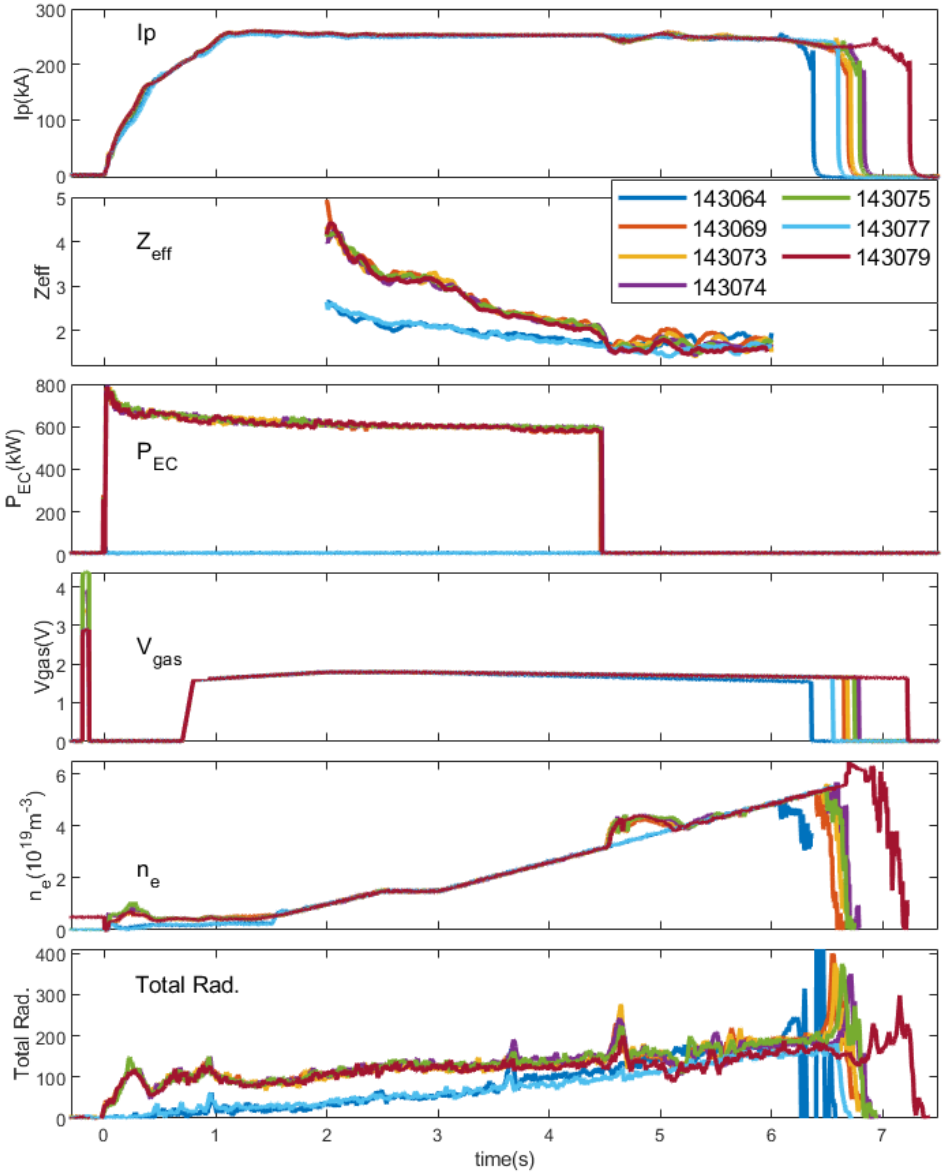

FIG. 2. **Time histories of key parameters in density limit discharges with varied ECRH power**. I_p: plasma current; Zeff: averaged effective charge number; P_{EC}: injected ECRH power; V_{gas}: voltage applied to control gas puffing, which is positively correlated with the puffed gas amount; n_e: line-averaged electron density measured using the central chord of HCN interferometer; Total Rad.: relative intensity of total radiation measured using bolometer.

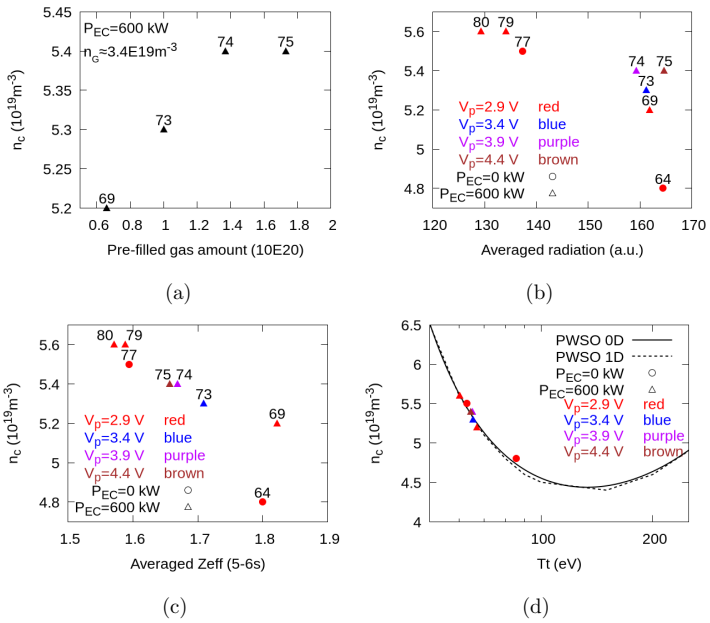

FIG. 3. **Relationship between the density limit and several key parameters in discharges with varying pre-filled gas pressure levels during the start-up phase and two different ECRH powers**. The density limit n_c is shown as a function of: (a) the corresponding particle number of pre-filled gas (D_2) with an ECRH power of about 600 kW; (b) the time-averaged relative radiation in time interval (5s-6s); (c) the time-averaged effective charge number Z_{eff}; (d) the time-averaged plasma temperature near the lower outer divertor T_t. The number label next to each symbol denotes the last 2 digits of the shot number 1430xx. The solid and dashed line in (d) represent the prediction of PWSO 0D and 1D model, respectively.

onto the wall targets, which can be modeled as [8, 11]

$$\alpha = \frac{f\lambda}{aD_{\perp}T_t} I\left(T_t\right) \int_0^a rn(r) R_{\text{coe}} \mathrm{d}r \tag{2}$$

Here a is the wall radius in unit of meter, n is the electron density in unit of m^{-3}, $D_{\perp}$ is the perpendicular diffusion coefficient in unit of $\mathrm{m}^2 \cdot \mathrm{s}^{-1}$, T_t is the plasma temperature around the target plate location in unit of eV, f is the fraction of the sputtered atoms that reach the main plasma and become ionized at a distance λ inwards from the plasma target location, R_{coe} is the impurity radiation rate coefficient in unit of $\mathrm{eV} \cdot \mathrm{s}^{-1} \cdot \mathrm{m}^3$, and $I\left(T_t\right)$ is an average of the yield function of impurity $Y\left(E\right)$ over the energies of the impinging particles

$$I\left(T_t\right) = \sqrt{\frac{m}{2\pi T_t}} \int_0^{\infty} Y\left(\frac{mv^2}{2} + \gamma T_t\right) \exp\frac{-mv^2}{2T_t}\, \mathrm{d}v \tag{3}$$

where γ is the total energy transmission coefficient [17], γT_t is a measure of the Debye sheath height, and m is the ion mass. The fixed point of Eq. (1) $R = R_+$ corresponds to the plasma-wall self-organization equilibrium, which becomes unstable for $\alpha > 1$ as predicted from Eq. (1). So the threshold $\alpha = 1$ establishes an upper radiation density limit

$$n_c = \frac{2D_{\perp}}{f\lambda R_{\text{coe}}} \frac{T_t}{I\left(T_t\right) a} \tag{4}$$

that can be reached for a ratio of total radiated power to total input power as low as 1/2 [8]. There are two density limit basins of PWSO. One is the regime of density limit corresponding to the higher temperature of target, whereas the other is the regime of density freedom corresponding to the lower temperature of target, in particular in machines where the target plates are made of high-Z materials [8, 11]. For high-discharge-number impurity, such as tungsten, the yield function $Y(E)$ is dominated by the physical sputtering. So in the following calculation, the contribution from chemical sputtering is ignored. The empirical formula for $Y(E)$ at normal incidence are provided in Eq. (15) of [18] for physical sputtering

$$Y_{\text{phy}}(E) = 0.042 \frac{Q\left(Z_2\right) \alpha^* \left(M_2/M_1\right)}{U_s} \frac{S_n(E)}{1 + \Gamma k_e \left(\epsilon\right)^{0.3}} \times \left[1 - \sqrt{\frac{E_{\text{th}}}{E}}\right]^s \tag{5}$$

where the meanings of coefficients and variables can be found in [18] and [13].

According to the impurity radiation measured using the EUV spectrometer, the main impurities in the plasma include carbon and tungsten, which is sputtered from the divertor target plates. Previous experimental and modeling results demonstrate that carbon is a dominant impurity causing tungsten sputtering in L-mode plasmas on EAST [19]. Thus in the calculation of PWSO model, we consider the sputtering of tungsten by carbon ions. The impurity radiation rate $R_{\mathrm{coe,W}}$ is estimated to be a constant value $10^{-30}/(1.602 \times 10^{-19})$ eV·s^{-1}·m^3 based on the simulation results using the FLYCHK code [20]. We further assume that the perpendicular diffusion coefficient $D_\perp$ of target impurities is 3 m^{2}s^{-1}, and one percent of the sputtered atoms penetrate the main plasma, undergoing ionization at a distance $\lambda = 0.01$ m away from the target. A maximal projectile energy E of 740 keV, well above the thermal energy, is used as the upper limit in the integral in Eq. (3). For these experiments on EAST, the radius $a = 0.45$ m. With the above EAST parameters, the PWSO 0D model predicts that there are two density limit basins. The EAST experimental results are located in the density-free regime, exceeding the Greenwald density limit (Fig. 3d), and are in good agreement with the PWSO 0D model prediction. The PWSO 1D model, which incorporates the evolution equations of radiation power and temperature toward a PWSO equilibrium, yields predictions similar to those of the PWSO 0D model, as shown in Fig. 3d. Further details of the 1D model calculation are provided in [13].

4. DISCUSSION

These EAST experiments show that a moderate increase of ECRH power and/or pre-filled gas pressure at start-up enhances the density limit at the flat-top phase of discharge. This enhancement of the density limit is related to the lower plasma temperature around the divertor target and can be explained using the plasma-wall self-organization model. Whereas the experimental results on J-TEXT tokamak are found to locate in the density limit basin predicted by the PWSO theory [11], the EAST experimental results are located in the density-free regime, which further validate the PWSO theory and highlight the significance of high-Z materials in the targets for accessing the enhanced density limit and the density-free regime as expected in [8]. These experiments demonstrate and validate a practical scheme to raise the density limit, which can be extended and applied to other magnetic confinement fusion devices in the future.

Because new start-up scenarios are prone to disruptions, we operated at relatively low current to prevent machine damage and to ensure the safe application of high ECRH power. From a modeling perspective, the PWSO-based scheme for enhancing the density limit is applicable to both low- and high-current discharges. The present work demonstrates its validity under low-current conditions, and extend the validation to higher current regimes is a direction of future studies.

The target temperatures is a bit high ($>$ 50 eV) in general. The high target temperatures are likely due to the narrowing heat-flux distribution, as indicated from the diagnostic data of target temperature. The target temperature T_t is obtained from Langmuir probe measurements near the divertor, with 16 channels covering different poloidal positions. Among the 16 channels, five of them (marked by arrows in Fig. 4) show high values in the 5–6 s interval, and T_t is taken as the average over these five channels. As seen in Fig. 4, before 4 s the temperature T_t remains relatively low ($\sim$50 eV) and fairly uniform, whereas during the 5–6 s interval T_t becomes higher only at 5 channels, likely due to the narrowing heat-flux distribution. This narrowing is consistent with the reconstructed q profile which decreases from 2s to 5s, implying a lower heat flux decay length λ_q, as shown in Fig. 5

Assuming that the temperatures at the separatrix are above the target temperatures, these temperatures are so high that MARFE cannot occur. Instead, the density limit disruption here results from the feedback loop between impurity radiation and plasma–wall interaction, which can drive a radiative instability independent of the MARFE onset. Experimentally, in the disruptive cases we studied, clear signatures of both thermal quench (Fig. 7R in this reply) and the subsequent current quench (Fig. 2) follow the excessive growth of radiation from impurity ion out of target sputtering, thus confirming the PWSO model. Both the experimental results and PWSO predictions suggest that an even higher density limit can be achieved at lower target temperatures, provided that a detachment can simultaneously take place so that the separatrix temperature would remain sufficiently high and an MARFE can be avoided as well.

In conclusion, we report on the experimental results on EAST tokamak that have achieved line-averaged electron density in the range of 1.3 to 1.65 Greenwald density limit, and our quantitative comparison with the predictions of plasma-wall self-organization theory that shows good agreement. Increasing ECRH power and/or pre-filled gas

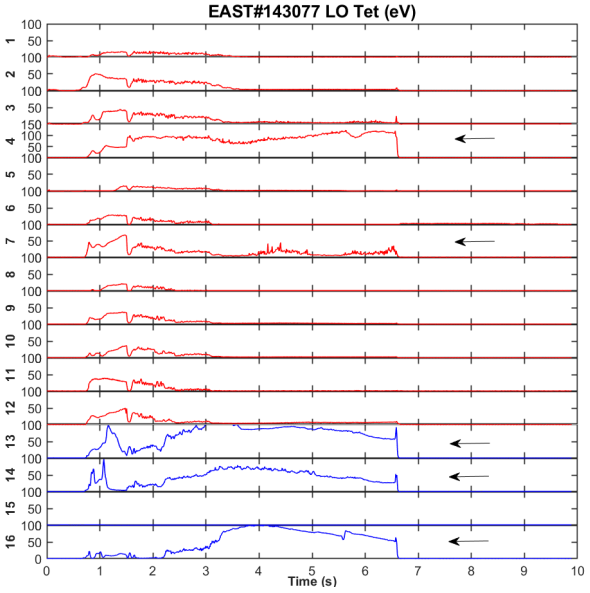

FIG. 4. Electron temperatures as functions of time measured using a 16-channel Langmuir probe on the lower-outer divertor. Different channels represent different poloidal positions on the divertor.

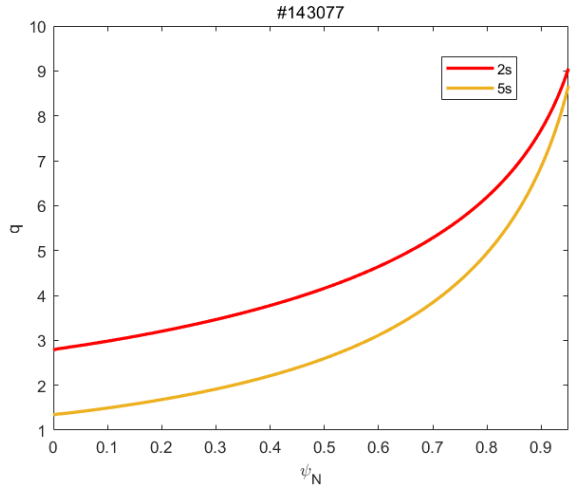

FIG. 5. Safety factor (q) profiles as functions of the normalized poloidal magnetic flux $\psi_{\rm N}$ of discharge #143077 reconstructed using EFIT code at 5s and 6s time points.

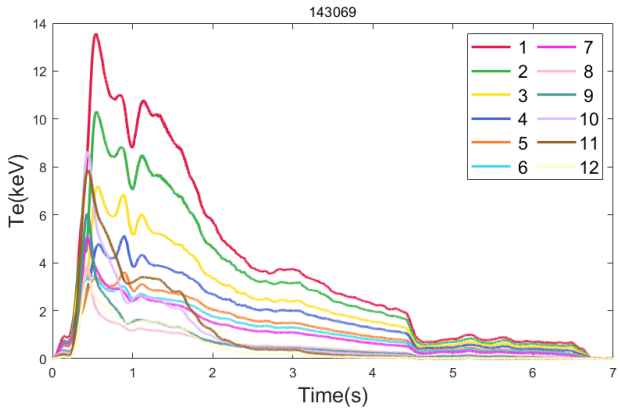

FIG. 6. Time evolution of electron temperatures (T_e) at various radial locations on middle plane (Z=0) measured using Thomson scattering for discharge #143069. The labels 1,. . . ,12 represent different horizontal positions, from core to edge, R=1.92, 1.95,. . . ,2.26, 2.29 m.

pressure are confirmed to lead to lower plasma temperature around the divertor target and higher density limit at the flat top. The experiments are found to locate in the density-free regime of PWSO model from both 0D and 1D predictions. These results demonstrate the potential of a practical scheme for substantially increasing the tokamak density limit. Although ultimately it is the triple product $nT\tau_E$ that governs the fusion ignition condition, the breaking of Greenwald density limit and the successful access to the density-free regime as demonstrated in this work opens a promising path advancing towards achieving the fusion ignition condition.

ACKNOWLEDGEMENTS

This work is supported by the National MCF Energy R&D Program of China under Grant Nos. 2019YFE03050004 and 2022YFE03020004, the U.S. Department of Energy Grant No. DE-FG02-86ER53218, and the Hubei International Science and Technology Cooperation Project under Grant No. 2022EHB003.

REFERENCES

[1] M. Greenwald. "Density limits in toroidal plasmas". In: *Plasma Physics and Controlled Fusion* 44.8 (2002), R27–R53.

[2] A. Huber et al. "Comparative H-mode density limit studies in JET and AUG". In: *Nuclear Materials and Energy* 12 (2013), pp. 100–110.

[3] P. Manz et al. "The power dependence of the maximum achievable H-mode and (disruptive) L-mode separatrix density in ASDEX Upgrade". In: *Nuclear Fusion* 63.7 (2023), p. 076026.

[4] P. Zanca et al. "A power-balance model of the density limit in fusion plasmas: application to the L-mode tokamak". In: *Nuclear Fusion* 59.12 (2019), p. 126011.

[5] P. Zanca et al. "A power-balance model for the L-mode radiative density limit in fusion plasmas". In: *Plasma Physics and Controlled Fusion* 64.5 (2022), p. 054006.

[6] G. Pucella et al. "Density limit experiments on FTU". In: *Nuclear Fusion* 53.8 (2013), p. 083002.

[7] S.Y. Ding et al. "A high-density and high-confinement tokamak plasma regime for fusion energy". In: *Nature* 629 (2024), pp. 555–560.

[8] D.F. Escande, F. Sattin, and P. Zanca. "Plasma-wall self-organization in magnetic fusion". In: *Nuclear Fusion* 62.2 (2022), p. 026001.

[9] R.C. Wolf et al. "Performance of Wendelstein 7-X stellarator plasmas during the first divertor operation phase". In: *Physics of Plasmas* 26.8 (2019), p. 082504.

[10] P. Zanca et al. "A unified model of density limit in fusion plasmas". In: *Nuclear Fusion* 57.5 (2017), p. 056010.

[11] J.X. Liu et al. "Validation of the plasma-wall self-organization model for density limit in ECRH-assisted start-up of Ohmic discharges on J-TEXT". In: *Nuclear Fusion* 63.9 (2023), p. 096009.

[12] Y.H. Ding et al. "Overview of the recent experimental research on the J-TEXT tokamak". In: *Nuclear Fusion* 64.11 (2024), p. 112005.

[13] J.X. Liu et al. *Increasing the density limit with ECRH-assisted Ohmic start-up on EAST*. 2025. arXiv: 2505.02710.

[14] J.L. Hou et al. "First results of high density H-mode operation in metal-wall EAST tokamak". In: *Results in Physics* 56 (2024), p. 107260.

[15] W.B. Liu et al. "ECW assisted plasma startup with low toroidal electric field and full metal wall in EAST superconducting tokamak". In: *Nuclear Fusion* 64.12 (2024), p. 126072.

[16] N. Asakura. "Wall pumping and saturation in divertor tokamaks". In: *Plasma Physics and Controlled Fusion* 46.12B (2004), B335–B347.

[17] P.C. Stangeby. *The Plasma Boundary of Magnetic Fusion Devices*. Boca Raton: CRC Press, 2000.

[18] Y. Yamamura and H. Tawara. "Energy dependence of ion-induced sputtering yields from monatomic solids at normal incidence". In: *Atomic Data and Nuclear Data Tables* 62.2 (1996), pp. 149–253.

[19] H. Xie et al. "ERO modelling of tungsten erosion and re-deposition in EAST L mode discharges". In: *Physics of Plasmas* 24.9 (2017), p. 092512.

[20] H.K. Chung et al. "FLYCHK: Generalized population kinetics and spectral model for rapid spectroscopic analysis for all elements". In: *High Energy Density Physics* 1.1 (2005), pp. 3–12.